Raman Spectroscopy

Deutsche Ausgabe: DOI: 10.1002/ange.201603758
Internationale Ausgabe: DOI: 10.1002/anie.201603758

3D SERS Imaging Using Chemically Synthesized Highly Symmetric Nanoporous Silver Microparticles

*Sanpon Vantasin, Wei Ji, Yoshito Tanaka, Yasutaka Kitahama, Mengfan Wang, Kanet Wongravee, Harnchana Gatemala, Sanong Ekgasit, and Yukihiro Ozaki**

Abstract: *3D surface-enhanced Raman scattering (SERS) imaging with highly symmetric 3D silver microparticles as a SERS substrate was developed. Although the synthesis method is purely chemical and does not involve lithography, the synthesized nanoporous silver microparticles possess a regular hexapod shape and octahedral symmetry. By using p-aminothiophenol (PATP) as a probe molecule, the 3D enhancement patterns of the particles were shown to be very regular and predictable, resembling the particle shape and exhibiting symmetry. An application to the detection of 3D inhomogeneity in a polymer blend, which relies on the predictable enhancement pattern of the substrate, is presented. 3D SERS imaging using the substrate also provides an improvement in spatial resolution along the Z axis, which is a challenge for Raman measurement in polymers, especially layered polymeric systems.*

Surface-enhanced Raman scattering (SERS) spectroscopy is a highly sensitive and selective technique that provides rich molecular information. SERS has been widely used in various applications, including life sciences and materials sciences.[1–3] Recently, three-dimensional SERS substrates have been developed by many research groups and have been shown to possess promising signal quality owing to their exponentially large surface area and substantial number of hotspots from the additional third dimension.[4–6] However, almost all of the 3D SERS substrate studies only present point-by-point measurement or 2D SERS imaging, which does not fully utilize the three-dimensional nature of the substrates. To the best of our knowledge, only one study demonstrates a breakthrough of the 2D limitation with 3D SERS imaging on a 3D SERS substrate,[7] and reported very interesting applications in the 3D encoding of digital data. Even so, the study used lithographed micropyramids decorated with Ag nanocubes as a SERS substrate, which caused the enhancing surface to be a topologically extruded 2D plane rather than a proper 3D object. It is worthy to note that nanoparticle aggregates[8] or 3D-movement nanoparticle tracking[9] can be utilized to perform 3D SERS imaging in cells, which enables remarkable investigations of intracellular pathways. However, these techniques have limited applications in materials science since the aggregation and 3D motion of nanoparticles are semi-random, and thus the enhancement pattern is unpredictable. The present study uses chemically synthesized symmetric silver microparticles to further the potential of 3D SERS imaging in creative applications, such as dispersible 3D SERS probes for embedding into samples, which allows the use of much lower laser power compared to that of normal 3D Raman spectroscopy while also providing improved spatial resolution. The objective is not to claim superiority in the enhancement factor of the 3D SERS substrate over previously reported substrates but to provide an alternative substrate for unexplored applications.

The nanoporous silver microstructures in this study were synthesized by in-place galvanic reduction of a AgCl template, as described in the Experimental Section. The SEM image in Figure 1 A shows a regular hexapod structure with octahedral symmetry (where each leg is of the same length and is 90° from adjacent legs). The nanopores, which act as hotspots, are presented in Figure 1 B, with an average pore

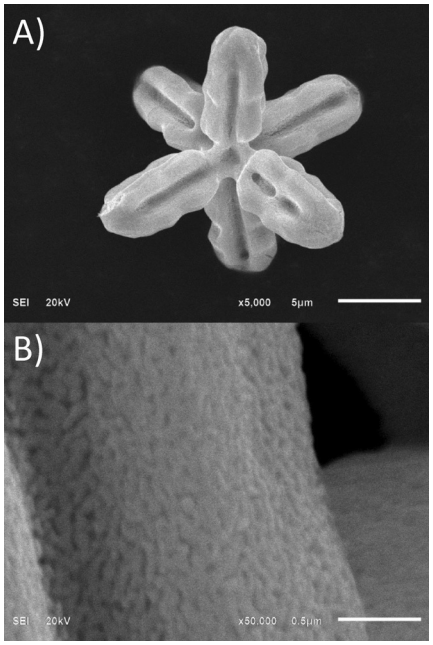

Figure 1. SEM images of nanoporous silver microstructures showing A) the overall hexapod shape (scale bar: 5 μm), and B) the nanopores (scale bar: 0.5 μm).

[*] S. Vantasin, Dr. W. Ji, Dr. Y. Tanaka, Dr. Y. Kitahama, M. Wang, Prof. Dr. Y. Ozaki
Department of Chemistry, School of Science and Technology
Kwansei Gakuen University
2-1 Gakuen, Sanda, Hyogo, 669-1337 (Japan)
E-mail: ozaki@kwansei.ac.jp
Dr. K. Wongravee, Dr. H. Gatemala, Prof. Dr. S. Ekgasit
Department of Chemistry, Faculty of Science
Chulalongkorn University
254 Phayathai Rd., Pathumwan, Bangkok 10330 (Thailand)

Supporting information for this article can be found under: http://dx.doi.org/10.1002/anie.201603758.

size of approximately 60 nm. This pore size should allow small molecules, such as SERS probe molecules, to travel deep inside the cavities of the particles instead of just on the outer surface. In our previous study, the Raman enhancement uniformity among areas in a single hexapod particle was evaluated to be within an order of magnitude.[10] The study also confirmed the 99.9% purity of silver throughout the structures by energy-dispersive X-ray spectroscopy (EDS).

An advantage of an octahedrally symmetric structure is that when the silver microparticles lie on a flat surface, they will always be pulled downwards by gravity and will rest on three legs, regardless of orientation. The other three legs will point upward at 45° from the flat surface plane, as shown in Figure 1 A. Due to the symmetry, every hexapod particle will have an apparent leg-to-adjacent-leg angle of 30° and leg-to-opposite-leg size of 2cos(leg length) when viwed from the Z axis (and from all directions equivalent to the Z axis in octahedral symmetry). Particle orientations similar to that in Figure 1 A almost always occur for hexapod particles, and thus it is an easy-to-find target. The ability to differentiate the lower legs from the upper legs when viewed from above is a crucial factor for 3D SERS imaging.

Figure 2 A shows a SERS spectrum of *p*-aminothiophenol (PATP) from the center of the particle in Figure 2 B. PATP is a well-known and important SERS probe because it can adsorb very well onto silver, giving strong SERS signals.[11,12] In our previous study, PATP with a concentration as low as 10^{-8} M could be detected by SERS when using similar hexapod silver microstructures.[10] Figure 2 C–E show 3D SERS imaging from the peak area of the 1074 cm^{-1} band. The band was selected because it is a simple Raman band that can be unambiguously assigned to the a_1 mode C–S stretching of PATP in the C_{2v} point group.[11] The enhancement pattern is easily predictable, since the top-view enhancement mapping in Figure 2 C closely resembles the particle shape in Figure 2 B. The XY slices shown in Figure 2 E display an obvious pattern, as the hotspots are gradually translated from the upper leg positions to the lower leg positions. Figure 2 D and E both indicate that the SERS enhancements appear to be slightly smaller for the lower legs than for the upper legs. This is most likely due to the shadowing effect, since the upper legs block some part of the incoming laser and outgoing Raman signal from the lower legs. This hypothesis can be tested by performing 3D SERS imaging on many hexapod particles, since all other measured particles show similar trends in the upper leg/lower leg signal. The symmetry and regularity in the structure, along with the predictable enhancement pattern of this 3D SERS substrate, is crucial in sensing applications; if there are irregularities or large differences in SERS signals from each equivalent leg of the hexapod, it is certain that the differences come from external factors (e.g., sample inhomogeneity) and not the particle itself.

Polarization studies show that the polarization of excitation laser does not affect the enhancement pattern of the nanoporous silver particles. (see the Supporting Information.) This polarization independence is useful, since it also means that there are no complications due to rotation of the particles in the XY plane.

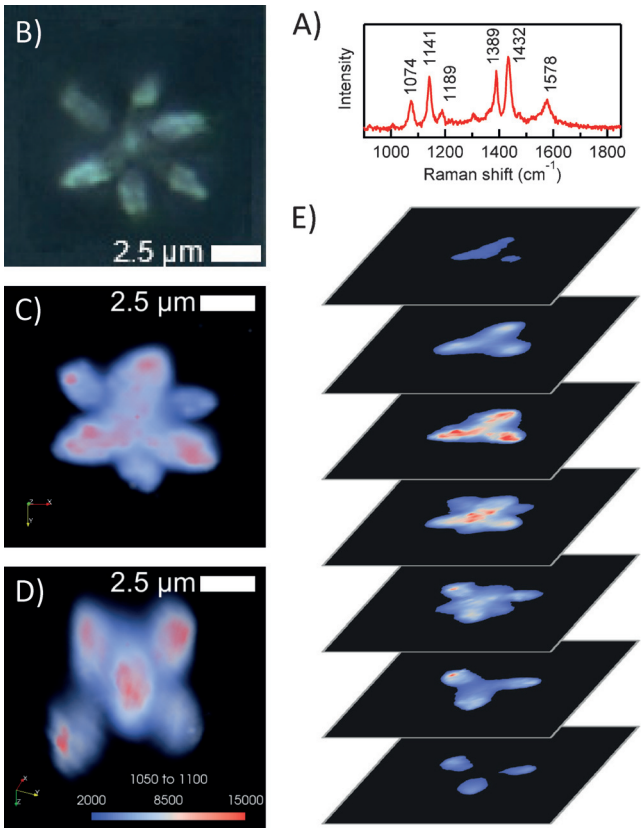

Figure 2. A) A SERS spectrum of PATP from the center of a hexapod silver microstructure. B) An optical microscopy image of the particle. C, D) Top and diagonal views of 3D SERS images measured from the particle shown in (B), and rendered using the peak area from the PATP a_1 mode at 1074 cm^{-1}. E) Examples of 2D slices in the Z axis of (B). Only one in five slices (corresponding to a 1.5 µm distance) are shown. Noted that (C), (D) and (E) use the same color scale.

A possible application of this 3D substrate is demonstrated by embedding the microparticles into polymers. Since this substrate has inherent SERS activity from its uniform nanopores and requires neither nanoparticle decoration nor aggregation, there is no risk of enhancement loss through the detachment of nanoparticles. Therefore, it may be embedded in various environments while retaining its SERS activity. In contrast to plane-extruding lithography-type 3D substrates, which are bound to the underlying surface, this substrate can go anywhere in the sample, even at the volume near the top of the sample. For example, the upper legs of the silver hexapod in Figure 3 A are located around 3 µm under the polymer surface, and the particle bottom is still several micrometers above the underlying glass slide (see the Figure 3 B). In this experiment, a 1:1 blend of poly(3-hydroxybutyrate) (PHB) and poly(D,L)lactic acid (PDLLA) was used. Both polymers are popular biodegradable polymers, and blending them together improves their physical properties over those of the original polymers.[13–15] Owing to presence of the same functional groups (Figure S3 in the Supporting Information), the interaction between each polymer with silver should be very similar, and variations in the measured SERS spectra should come from the polymer distribution.

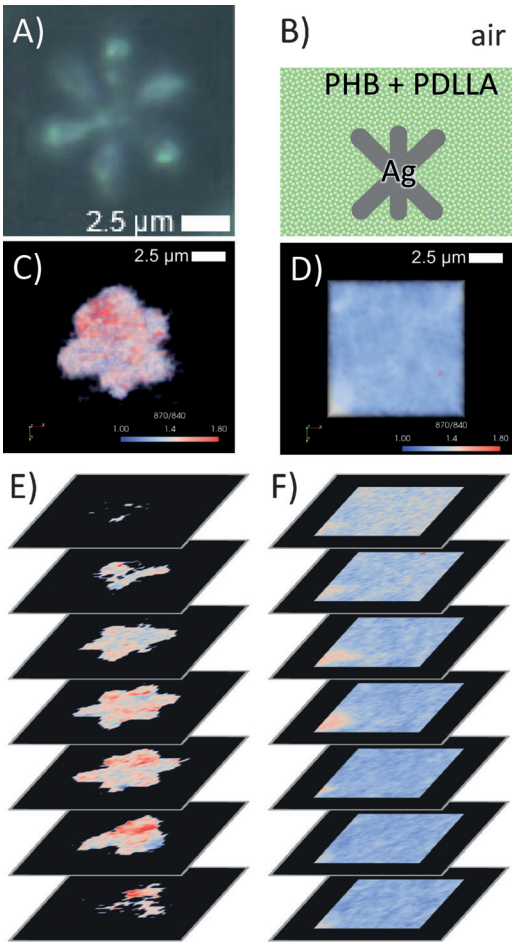

Figure 3. A silver microparticle in a PHB/PDLLA polymer blend. A) An optical image. B) A side-view scheme. C) 3D SERS imaging on the particle showing the 870/840 cm^{-1} peak ratio. D) 3D Raman imaging showing the same peak ratio but on the polymer outside of the particle. E, F) Examples of 2D slices along the *Z* axis from (C) and (D), respectively. Only one in five slices (corresponding to 1.0 µm distance) are shown.

Figure 3 C, E presents a top-view image and 2D slices of 3D SERS imaging of the particle shown in Figure 3 A, with the color representing the ratio of the 870/840 cm^{-1} peak areas. The peaks originate from the C–COO stretching modes of PDLLA and PHB,[13] respectively. SERS spectra with the peaks are shown in Figure S4 of the Supporting Information. The enhancement is very low compared to that of PATP because the carbonyl group of the polymers does not adsorb well onto the silver particle. Nevertheless, the 3D image based the on the peak area ratio shows a high value in some microscale areas, which could be interpreted as an inhomogeneity in the blend (in which the area consists of more PDLLA content). Actually, normal 3D Raman imaging can also be used to probe the inhomogeneity in polymers,[16,17] but it is well known that conventional Raman spectroscopy in polymers suffers from a limitation in spatial resolution owing to refraction of light at polymer interface, especially in the Z axis, which could be as bad as 20 µm.[18,19] It can be clearly seen in the 3D Raman images of the nearby polymer without the silver structure (Figure 3 D and F) that the inhomogeneity is not resolved very well. This is due to the worsened resolution in the Z axis, which causes the spectrum from every point to be similar to that for the bulk average. With the symmetric 3D SERS substrate, the probing volume for each measurement point is constrained to the smaller volume near the corresponding surface of the silver particle in the Z axis, thus improving Z-axis spatial resolution. Therefore the microscale inhomogeneity can be resolved.

The potential of this method for improving spatial resolution in the Z axis can be demonstrated in double-layered polymeric systems. Hexapod silver particles were embedded into the interface between polyvinylpyrrolidone (PVP) and polystyrene (PS; Figure 4 A, B). Similar to the polymer blend system, the low enhancement from poor adsorption results in noisy 3D SERS images. Nevertheless, when using the peak area ratio between PS ring-mode vibration[20] (1002 cm^{-1}) and PVP C–C ring breathing[21] (933 cm^{-1}), a partition of the polymers can be seen. The top- and side-view 3D SERS images in Figure 4 C and D show high PS/PVP peak area ratios on the upper legs of the particle and low ratios on the lower legs. This cannot be replicated in normal 3D Raman imaging (Figure S6) because the gradient of the peak area ratio is low. More quantitative information can be acquired by considering averaged spectra at each depth. The particle appears flatter than normal in side-view (Figure 4 D) due to refraction (objects in a medium with high refractive index have a smaller apparent height when viewed from above). Figure 4 E, F clearly show that the contrast between at 1.2 and 2.4 µm depth in 3D SERS imaging is much better than in normal 3D Raman imaging. Figure 4 G illustrates a decrease of the PS/PVP peak area ratio to 20 % of the maximum for just ca. 1 µm of depth change, in contrast to several micrometers required in normal 3D Raman imaging (See Figure S5 in Supporting Information for average spectra at each depth.). Noted that this resolution improvement in the Z axis overcomes the limitation from refraction at polymer interfaces. It does not exceed the diffraction limit of light, which is approximately 580 nm in PS with this setup. Surface chemistry certainly affects the SERS signal. SERS spectra of PS and PVP exhibit shifts for several peaks.[22,23] Fortunately, references suggest that the peaks used in this area ratio analysis barely shift at all.[22,23]

By using 3D SERS imaging, we characterized highly symmetric nonporous silver microparticles for their SERS properties in three dimensions. The results show that the substrate can provide volumetric SERS information. The enhancement pattern of the particles is very predictable since it correlates well with the particle shape. The polarization-independent enhancement pattern is an advantage, since it allows the substrate to be useful in every orientation. A potential application as an embedding SERS probe was demonstrated. In a PHB/PDLLA polymer blend, 3D SERS imaging on this symmetric nonporous silver structure can resolve microscale inhomogeneity of the blend. An improved spatial resolution in the Z axis was also illustrated in a double-layered polymeric system.

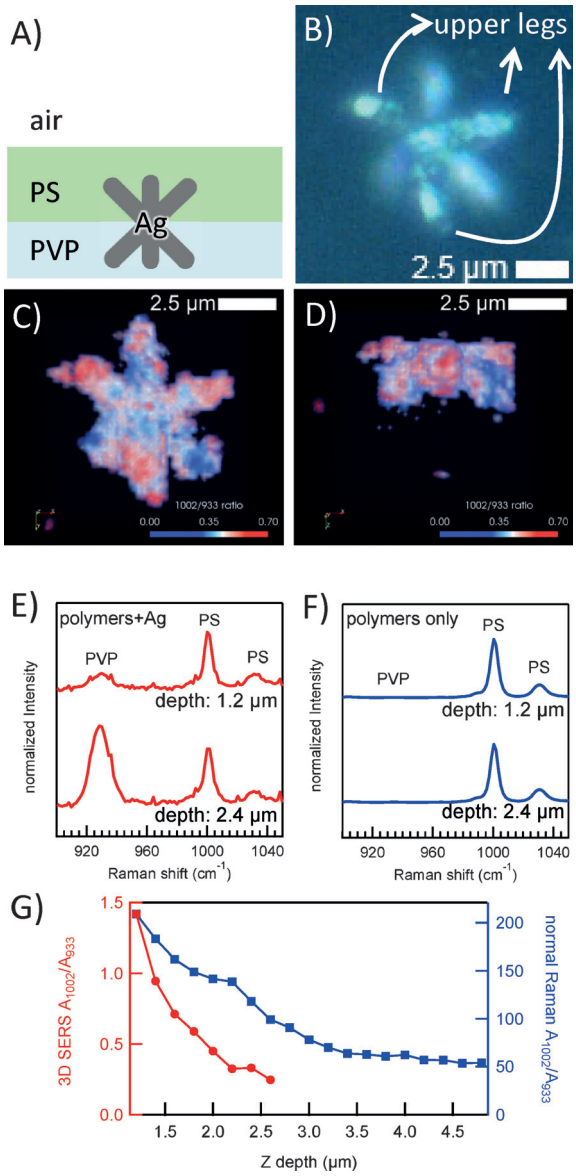

Figure 4. A) A scheme showing a silver particle embedded in double-layered polymers. B) An optical image of the silver particle in the polymers. C, D) Top- and side-view 3D SERS images constructed from the peak area ratio between the 1002 cm^{-1} band of PS and the 933 cm^{-1} band of PVP. E, F) Average spectra at depth 1.2 and 2.4 μm from 3D SERS imaging and normal 3D Raman imaging, respectively. G) The PS/PVP peak area ratio plotted against depth.

Experimental Section

Nanoporous silver microparticles with 3D symmetry were synthesized by a method slightly modified from that reported in our previous study.[10,24] $AgNO_3$ (0.1 M, 5 mL), NH_4OH (5.31 M, 4.7 mL), and NaCl (1 M, excess) were thoroughly mixed by vigorous stirring. The produced AgCl precipitate was washed, dried, and reduced with a Zn plate in NaCl solution (0.1 M) into hexapod Ag particles.

For SERS experiments, 1 mg of washed Ag microparticles was mixed with 10^{-3} M PATP in ethanol, 0.32 % PHB/0.32 % PDLLA in chloroform, or 1.25 % PVP in water for > 1 hour. The mixture was then dropped/casted and dried on a glass slide. For PATP, non-adsorbed molecules were washed with ethanol. For the polymer blend, repeated drops are needed for enough thickness. For the double-layer polymers, 1 % PS in 2-butanone was then casted over the PVP/Ag. The instrument for 3D SERS measurements was Renishaw Invia Raman spectrometer with 532 nm laser, 100X/0.85 NA objective lens, and *XYZ* stage controller. Mapping sizes are $45 \times 45 \times 45$ points for PATP and $41 \times 41 \times 41$ points for polymers, with 0.30 μm separations between points, except for 0.20 μm for the *Z* axis in polymers to compensate their high refractive index. The exposure time for each point was 0.4 s for PATP and 1.0 s for polymers. The laser power was 0.010 mW for SERS and 5.0 mW for normal 3D Raman imaging without Ag. Additional details are available in Supporting Information.

Acknowledgements

This research was partially supported by Adaptable & Seamless Technology Transfer Program through Target-driven R&D (A-Step) from Japan Science and Technology Agency and Ratchadaphiseksomphot Endowment Fund 2013 of Chulalongkorn University (CU-56-602-AM). Sanpon Vantasin would like to thank the Yoshida Scholarship Foundation for scholarship support.

Keywords: microparticles · polymers · Raman spectroscopy · silver · surface-enhanced Raman scattering

How to cite: *Angew. Chem. Int. Ed.* **2016**, *55*, 8391 – 8395
Angew. Chem. **2016**, *128*, 8531 – 8535

[1] K. Kneipp, M. Moskovits, H. Kneipp, Eds., *Surface-Enhanced Raman Scattering*, Springer, Berlin, **2006**.
[2] R. Aroca, *Surface-Enhanced Vibrational Spectroscopy: Aroca/Surface-Enhanced Vibrational Spectroscopy*, Wiley, Chichester, **2006**.
[3] G. McNay, D. Eustace, W. E. Smith, K. Faulds, D. Graham, *Appl. Spectrosc.* **2011**, *65*, 825 – 837.
[4] H. Tang, G. Meng, Q. Huang, Z. Zhang, Z. Huang, C. Zhu, *Adv. Funct. Mater.* **2012**, *22*, 218 – 224.
[5] S. Y. Lee, S.-H. Kim, M. P. Kim, H. C. Jeon, H. Kang, H. J. Kim, B. J. Kim, S.-M. Yang, *Chem. Mater.* **2013**, *25*, 2421 – 2426.
[6] H. Ko, S. Singamaneni, V. V. Tsukruk, *Small* **2008**, *4*, 1576 – 1599.
[7] Q. Zhang, Y. H. Lee, I. Y. Phang, C. K. Lee, X. Y. Ling, *Small* **2014**, *10*, 2703 – 2711.
[8] S. McAughtrie, K. Lau, K. Faulds, D. Graham, *Chem. Sci.* **2013**, *4*, 3566.
[9] K.-C. Huang, K. Bando, J. Ando, N. I. Smith, K. Fujita, S. Kawata, *Methods* **2014**, *68*, 348 – 353.
[10] K. Wongravee, H. Gatemala, C. Thammacharoen, S. Ekgasit, S. Vantasin, I. Tanabe, Y. Ozaki, *RSC Adv.* **2015**, *5*, 1391 – 1397.
[11] D.-Y. Wu, X.-M. Liu, Y.-F. Huang, B. Ren, X. Xu, Z.-Q. Tian, *J. Phys. Chem. C* **2009**, *113*, 18212 – 18222.
[12] K. Kim, K. L. Kim, D. Shin, J.-Y. Choi, K. S. Shin, *J. Phys. Chem. C* **2012**, *116*, 4774 – 4779.
[13] T. Furukawa, H. Sato, R. Murakami, J. Zhang, I. Noda, S. Ochiai, Y. Ozaki, *Polymer* **2006**, *47*, 3132 – 3140.
[14] E. Meaurio, E. Zuza, J.-R. Sarasua, *Macromolecules* **2005**, *38*, 9221 – 9228.
[15] W. Dong, P. Ma, S. Wang, M. Chen, X. Cai, Y. Zhang, *Polym. Degrad. Stab.* **2013**, *98*, 1549 – 1555.
[16] W. Smitthipong, R. Gadiou, L. Vidal, P. Wagner, M. Nardin, *Vib. Spectrosc.* **2008**, *46*, 8 – 13.
[17] R. A. Larsen, Y. Kubo, K. Akao, Y. Ohkubo, M. Yumoto, T. Nagoshi, *AIP Conf. Proc.*, AIP Publishing, **2010**, pp. 766 – 767.
[18] N. J. Everall, *Appl. Spectrosc.* **2000**, *54*, 1515 – 1520.
[19] N. J. Everall, *Appl. Spectrosc.* **2000**, *54*, 773 – 782.

[20] H. Lobo, J. V. Bonilla, *Handbook of Plastics Analysis*, CRC, Boca Raton, FL, **2003**.
[21] L. S. Taylor, F. W. Langkilde, G. Zografi, *J. Pharm. Sci.* **2001**, *90*, 888 – 901.
[22] J. R. Anema, A. G. Brolo, A. Felten, C. Bittencourt, *J. Raman Spectrosc.* **2010**, *41*, 745 – 751.
[23] M. A. Mahmoud, C. E. Tabor, M. A. El-Sayed, *J. Phys. Chem. C* **2009**, *113*, 5493 – 5501.
[24] H. Gatemala, C. Thammacharoen, S. Ekgasit, *CrystEngComm* **2014**, *16*, 6688.

Received: April 19, 2016
Published online: May 30, 2016

